Reducing the Computational Load of Attitude Estimation for Nano-Satellites using Integrated Measurements

Doğukan BENLİ[1)] , Halil Ersin SÖKEN[1)],
[1)] *Department of Aerospace Engineering, Middle East Technical University, Ankara, Turkey*
dogukan.benli@gmail.com

Computational power and efficiency of computer processors continue to improve with each passing year. This enables usage of less power for computing or more complex models for the embedded systems, especially in the aerospace industry. However, implementation of newer and more advanced technologies to the systems in the field or in production is not always easy. Therefore, it is still crucial to focus on more capable or efficient algorithms for these systems. The purpose of this research is to develop and compare methods that decrease the computational load of onboard attitude estimation algorithms that are using the Kalman Filter (KF) as the core algorithm. This is especially important for nano-satellites as they are limited both in terms of hardware and power consumption. In the literature, there exists methods that exploit the system model to reduce the complexity of matrix operations related to the operations of the KF. This paper focuses on reducing the number of KF updates without compromising the performance of the KF. This requires manipulation of the measurements, to get a pseudo-measurement of slower frequency. To this end, "integrated measurements" are suggested as a replacement for the original measurements.

Key Words: Attitude estimation, computational load, inertial navigation, integrated measurements, Kalman Filter

1. Overview

Inertial Navigation System's are used in a variety of applications to keep track of position, velocity and attitude of a vehicle. They are composed of integration algorithms that are usually fed by accelerometers and gyroscopes. However, due to erroneous nature of all sensors combined with the integration, the solutions drift. In order to keep these parameters bounded close to their truth values, estimation algorithms along with aiding measurements are utilized, most commonly a Kalman Filter (KF).

In nano-satellites, this approach is commonly used to keep track of the attitude. To that end, a triad of gyroscopes is used. With an integration scheme to keep track of attitude in mind, the attitude estimation problem can be divided into 2 parts. Initial attitude determination and continuous estimation of the concurrent attitude. This paper focuses on the latter, with the intent of decreasing the computational load of attitude estimation algorithms.

The attitude estimation algorithms usually rely on a KF as their estimator. It requires several matrix operations, which scales with the number of parameters required to be estimated. These computational requirements may be too heavy for a nanosatellite. Thus, the computational load must be considered[1)]. In the literature, there exists methods that reduce the complexity of these matrix operations, decreasing the computations required per estimation cycle[2)]. They usually deal with systems with very high number of states (Simultaneous Localization and Mapping, SLAM, problems)[3, 4)]. Their approach is to disregard the states that are not currently useful.

This paper focuses on reducing the number of estimation cycles to achieve an overall reduction in computational load via usage of integrated measurements and applied to nano-satellite attitude estimation problem. This approach is meant to be compatible with other approaches, complementing one another.

2. Attitude Estimation

Attitude estimation problem is usually divided into 2 components [5)]. First part is the initial attitude estimation, which is performed without any prior knowledge of the attitude. For the purposes of this paper, this is done by simply finding the rotation between 2 reference vectors and same 2 vectors measured in body coordinate system. This is a rough estimate considering the errors on the measurements. Second part is the continuous attitude estimation using the latest best attitude at hand. This algorithm feeds back to itself, further propagating its estimation. Most common application is the KF[6)] which is a commonly used optimal estimator.

After the initial attitude estimation is completed, inertial navigation algorithms will take hold and integrate gyroscope measurements to update the changes in attitude. This computed attitude will contain both the errors of the initial estimation and the integration of the sensor errors. A KF is used to estimate these errors. They can be compensated in the navigation algorithm accordingly.

For the purposes of this paper, Multiplicative Extended Kalman Filter (MEKF) will be used as the attitude estimation method. At its core, this method is a linearization of attitude around the current best attitude estimate, and attitude error is defined as a rotation between the estimate and the truth [7)].

Table 1 Characteristics for the modelled gyroscope

Repeatability Bias Error	1°/h
Instability Bias Error	10°/h
Noise	0.1°/√h
Output Frequency	1 Hz

Table 1 contains characteristics of a typical low-cost MEMS gyroscope[8, 9] that would typically be used for nano-satellites. The bias error alone could result in big attitude errors after hours of integration. In order to mitigate this, other available measurements can be used with the KF. For a Low Earth Orbit (LEO) satellite, these can be a triad of magnetometers and sun sensors[10]. Earth's magnetic field at satellites position and the position of the sun relative to the satellite would provide reference vectors in Earth Centered Inertial (ECI), while the sensors would provide measurements made in the body. Since the attitude of a spacecraft can be defined as the angles between these 2 coordinate systems, a relation can be formulated. This would provide a relationship between the difference of the reference and measurement vectors and the attitude error. This, along with the modelled sensor errors, would create a measurement model for the KF. KF can take these measurements and estimate attitude errors along with the sensor errors.

Table 2 Characteristics for the modelled sun sensor

Noise	1 mrad/√Hz
Output Frequency	1 Hz
Measurement cut-off by eclipse	

Table 3 Characteristics for the modelled magnetometer

Bias Error	4000 nT
Orthogonality Error	50 mrad
Scale Factor Error	0.1
Noise	830 nT/√Hz
Output Frequency	1 Hz

Table 2 and Table 3 shows the standard deviation of measurement errors on typical sensors of their own kinds [9, 10, 11]. These errors cannot be accounted in the initial attitude estimation, which leads to the continuous estimation approach.

3. Integrated Measurements Method

A regular approach to implementing the KF for the attitude estimation would utilize the measurements from the magnetometer and sun sensor as they become available. This would restrict the KF update frequency to their own, which is 1 Hz in this example. One could down sample the measurements and use them at a lower frequency to reduce the computational load, but that would come at the cost of performance. This paper suggests a manipulation on the measurements so that the KF can be slowed down without much effect on the performance of the filter.

Let $y_k^{B_k}$ be the measurement made at time t_k in the body frame of the satellite B_k. For an interval of N measurement cycles, the integral can be taken in a chosen frame of reference. Choosing B_N as the coordinate system for this purpose, which is the body coordinate system of the satellite at the end of the integration interval would yield the following:

Equation 1

$$Y_N = \int_{t_0}^{t_N} C_{B_t}^{B_N} y_t^{B_t} dt$$

Where, $C_{B_t}^{B_N}$ is the directional cosine matrix (DCM) that relates body coordinates at time t to at time t_N.

Since the measurements are discrete, this can be formulated in a discrete fashion, using a midpoint integration technique.

Equation 2

$$Y_N = \Delta t \sum_{i=1}^{N-1} C_{B_i}^{B_N} y_i^{B_i} + 0.5\left(C_{B_0}^{B_N} y_0^{B_0} + y_N^{B_N}\right)$$

Furthermore, since the attitude relation between the end of the interval is not known until the completion of the interval, the scheme can be converted into a recursive form to enable its computation at every time step rather than a bulk at the end, both saving memory and distributing compute time evenly.

Equation 3

$$Y_m = C_{m-1}^{m}\left(Y_{m-1} + 0.5 y_{m-1}^{B_{m-1}} \Delta t\right) + 0.5 y_m^{B_m} \Delta t,\ m = 1, .., N$$

Where, $Y_0 = 0$, Δt is the output interval of the sensor, and m is the counter for the steps to reach the integration interval.

This scheme distributes the computation of the discrete integral among the sensor measurement cycles rather than clumping all at the end. It is important for a real-time application for the computations to be evenly distributed in time for consistent performance.

KF can be designed for this new measurement with little modification. The errors present in the measurements y would be integrated into Y. This can be accounted by addition of a state that represents Y, the integrated measurement. This also greatly simplifies the measurement matrix, as the measurement becomes a state itself. As a result, both time propagation and measurement update portions of the KF can be slowed down to the frequency of the new measurements. Overall, this results in a reduction of computational load for the system.

However, it should be noted that this integration interval can not be increased forever. Assuming a variable attitude, the attitude estimation problem can be highly non-linear. The linearized KF can fail to represent the system properly within the given time interval. This will lead to a discrepancy between the actual errors of the estimation and the standard deviation estimated by the filter, along with the probability distribution of the errors.

4. Results

In this section, a KF that utilizes measurements directly (dubbed as regular KF) and a KF that uses the integrated measurements implementation will be compared. These approaches will be compared using a simple model with no states for sensor errors, then a complex model containing most commonly expected error states. The generated sensor errors will also correspond to the complexity to the model used.

4.1. Simple Model

Simple model contains 6 considered parameters. 3 for 3-dimensional attitude error, and 3 for gyroscope instability bias.

Truth data for gyroscopes, magnetometers[11, 12] and sun sensor were generated for a simple LEO satellite. Sun sensor and magnetometer data were finalized by adding only the noise errors specified in Table 2 and Table 3. Gyroscope measurements were finalized by adding all the errors specified in Table 1.

4.1.1. Regular KF

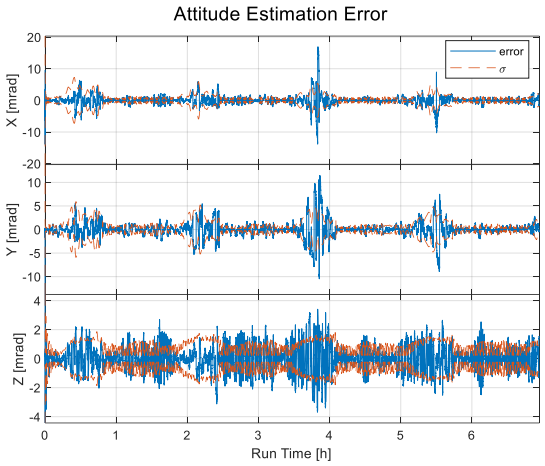

Figure 1 Attitude estimation error of regular KF

Figure 1 shows the attitude performance of a regular KF. While both magnetometer and sun sensor measurements are available, attitude uncertainty goes down below 1 mrad. Starting at about half hour mark, every 100 minutes the satellite goes behind the Earth and sun sensors stop providing directional measurements. This results in the uncertainty increasing up to 7 mrad for the worst case. The error remains mostly within the expected range in all cases.

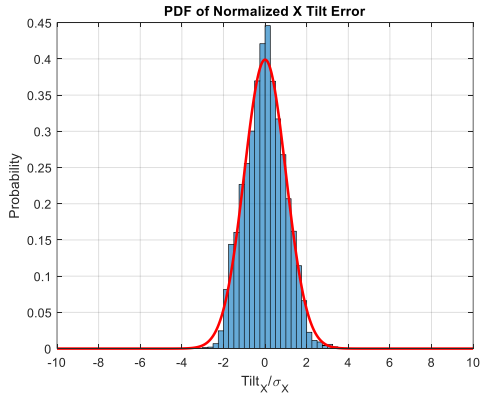

Figure 2 Probability Density Function (PDF) of x-axis angle error

Figure 2 shows the expected PDF of a gaussian distribution with a red line. Blue bars show the distribution of the realized error for a sample run. It confirms that the angle error is normally distributed.

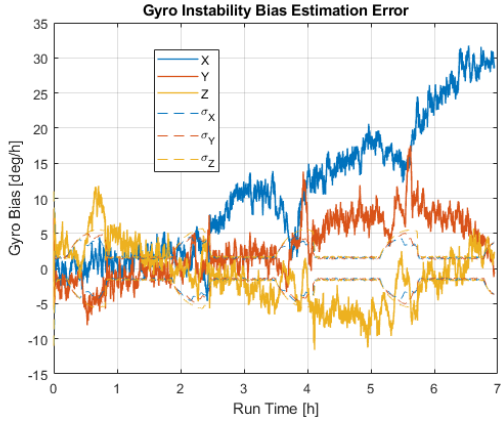

Figure 3 Gyro instability bias estimation error

Figure 3 shows the gyroscope instability bias estimation error for each axis. If both aiding measurements are cut-off completely, this estimation will not help in keeping the angle errors small. This is a flaw that occurs due to trying to estimate a randomly drifting gyro bias.

4.1.2 Integrated Measurements KF

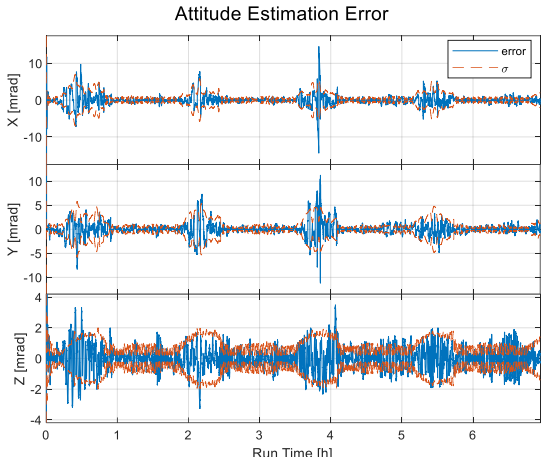

Figure 4 Attitude estimation error of 10s integrated measurements KF

Figure 4 shows the attitude estimation error of the KF that utilizes integrated measurements method for an interval of 10 seconds. The quality of attitude estimation is on par with that of the regular KF approach.

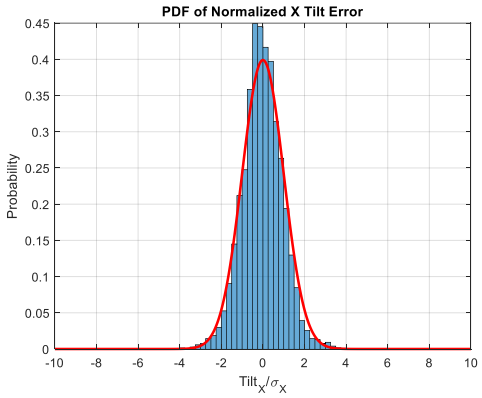

Figure 5 PDF of x-axis angle error for 10s integrated measurements KF

Figure 5 shows that the distribution of the angle errors has remained gaussian. If the integration interval is expanded, this distribution may slowly decay until divergence.

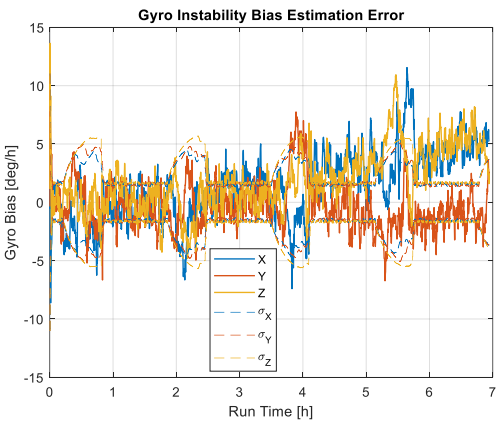

Figure 6 Gyro instability bias estimation error for 10s integrated measurements KF

Figure 6 shows an improvement in the estimation of a drifting gyroscope bias. The error remains within or in close proximity of the variance estimated by the KF.

A powerful desktop pc was used to compute attitude integrals with KF updates and feedback mechanisms for both the regular KF approach and integrated measurements KF approach, with a single core affinity. Both solution approaches were compared for a data of length of 7 hours. The speed up gained by the usage of 10 seconds of integrated measurements was measured to be a factor of 2.6x. This includes the overhead of numerical integrals brought with the new method. Comparisons of Figures 1-6 show that no performance has been lost in the process, and even some potential gains were achieved.

4.2. Complex Model

This model contains the 6 states from the simple model. On top of those the following states are added:

- 3 Magnetometer Bias Error States
- 3 Magnetometer Scale Factor Error States
- 3 Magnetometer Orthogonality Error States

This complex model amounts to total of 15 states for the regular KF approach. In order to implement the integrated measurements approach, 3 states must be added on top as *Integrated Magnetometer Error States*, totaling at 18 states. This increase in number of states will come at a computational cost.

Along with their model counterparts, all the error types specified in Table 1, Table 2 and Table 3 are added on top of their respective generated truth data. This constructs a more realistic set of measurements to test the proposed method to the traditional approach.

4.2.1 Regular KF with Complex Model

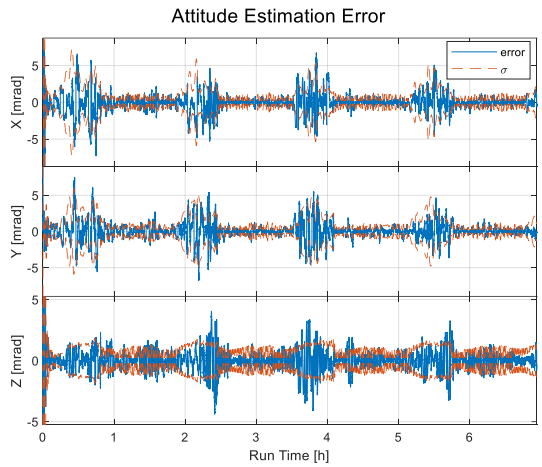

Figure 7 Attitude estimation error of regular KF with complex model

Figure 7 shows that the regular KF approach can still estimate the angles using complex model and errors at a similar, but slightly worse, level compared to the simple model and errors.

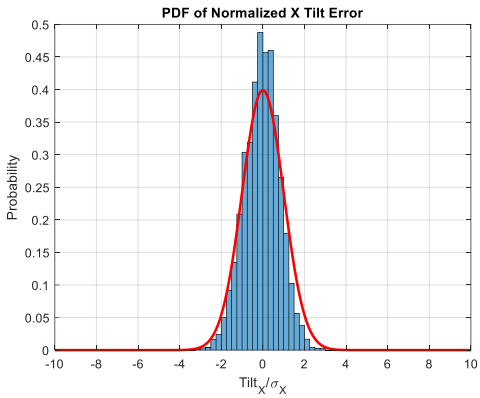

Figure 8 PDF of x-axis angle error with regular KF and complex model

Figure 8 shows that the integrity of the normal distribution is preserved. Regular KF is still able to estimate angles with the presence of the additional states and errors.

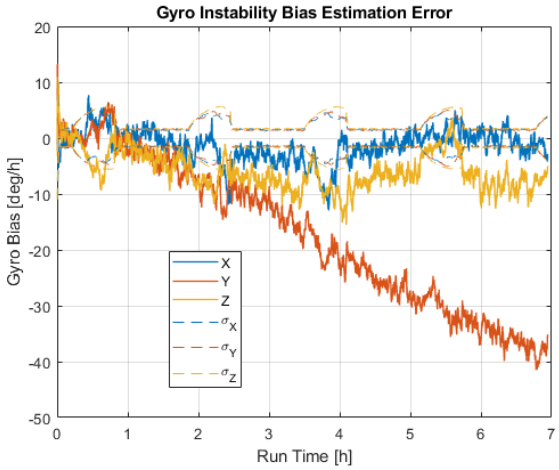

Figure 9 Gyro bias estimation error for regular KF with complex model

Figure 9 shows that while early estimates by the regular KF is within reason, it drifts away as time goes on. This flaw is identical to that of the simple model.

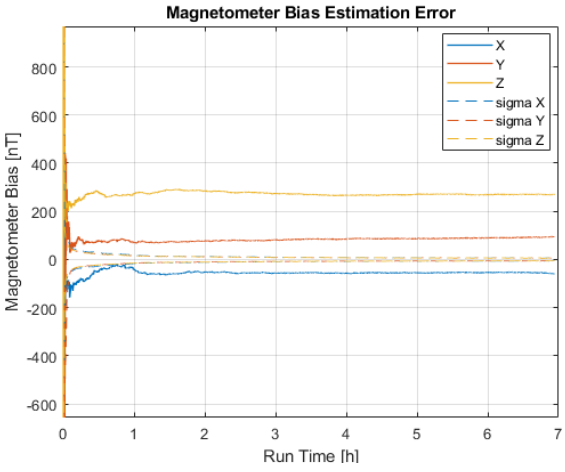

Figure 10 Magnetometer bias estimation error for regular KF with complex model

Figure 10 shows that the magnetometer bias can be reduced by an order of magnitude. The final estimation is a biased estimate.

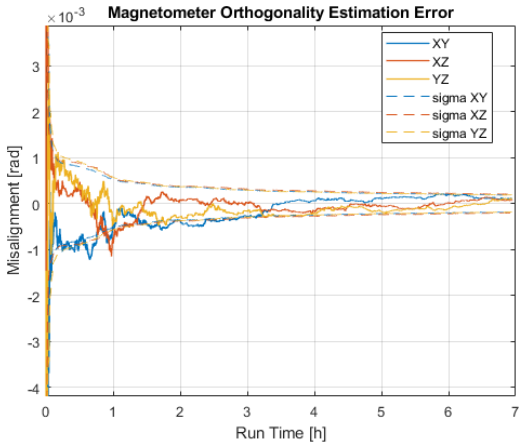

Figure 11 Magnetometer orthogonality estimation error for regular KF with complex model

Figure 11 shows that the orthogonality error is reduced from 50 mrad to below 0.5 mrad. For a LEO satellite, this error would be slightly lower than the magnetometer bias.

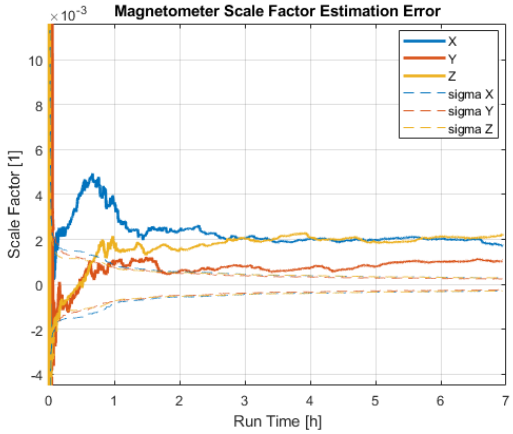

Figure 12 Magnetometer scale factor estimation error for regular KF with complex model

Figure 12 shows that the scale factor error is reduced from 10% to 0.2%. Before corrections, this error would be comparable to that of orthogonality error. Note that the final estimate is biased, as it was the case for the magnetometer bias estimate.

4.2.2 Integrated Measurements KF with Complex Model

In order to use the integrated measurements method with presence of errors on the actual measurement, the model for the KF must be expanded to include integrated error states. This is a current drawback with this method which will be investigated.

Note that the measurement noise (commonly denoted with R for KF applications) given to the integrated measurements KF has been tuned very slightly. All the errors are generated randomly so the tuning is not meant to compensate a sample case, but rather smooth out the initial large deviations. With a closed loop approach, these deviations may damage the accuracy of the linearized model used for the KF, resulting in slightly worse results.

The following results are obtained by integrating measurements for 10 seconds, and updating the KF at the end points of the integration cycles.

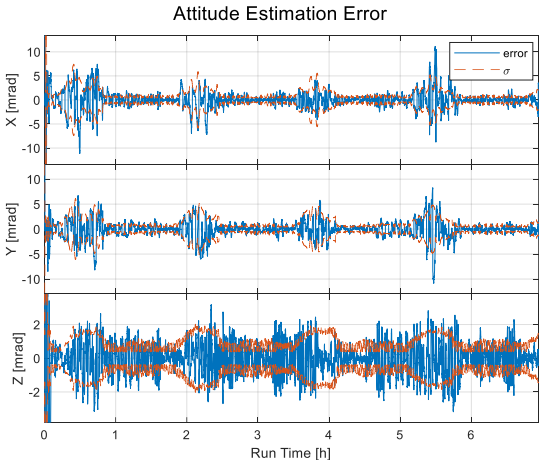

Figure 13 Attitude estimation error for 10s integrated measurements KF with complex model

Figure 13 shows that the quality of the angle estimates is comparable to that of the regular KF. The performance of the filter is not compromised.

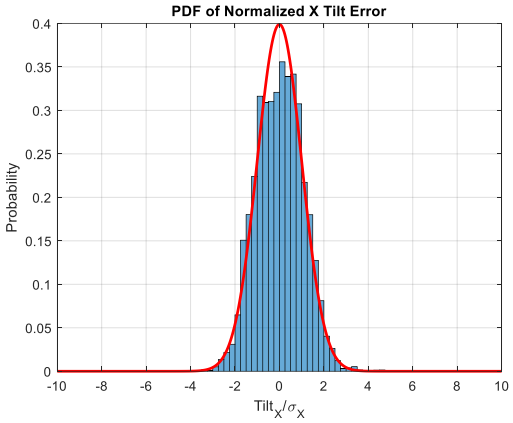

Figure 14 PDF of x-axis angle estimate error for 10s integrated measurements KF with complex model

Figure 14 shows that the actual error distribution is close to that of a normal distribution. However, peak of the distribution is slightly flattened. As the integration time is increased, the distribution is affected more and more until KF starts diverging.

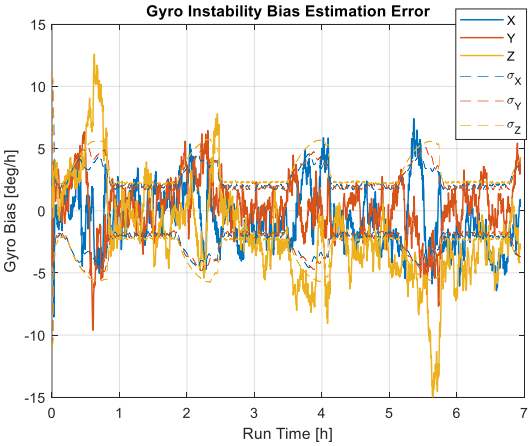

Figure 15 Gyroscope bias estimation error for integrated measurements KF with complex model

Figure 15 shows an improvement on the regular KF method for estimating drifting gyroscope bias errors. The errors are kept within the expected proximity of their variances throughout.

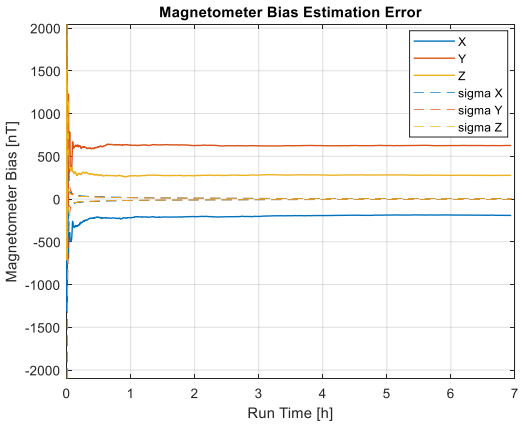

Figure 16 Magnetometer bias estimation error for integrated measurements KF with complex model

Figure 16 shows comparable magnetometer bias estimation errors to that of the regular KF. The performance is similar.

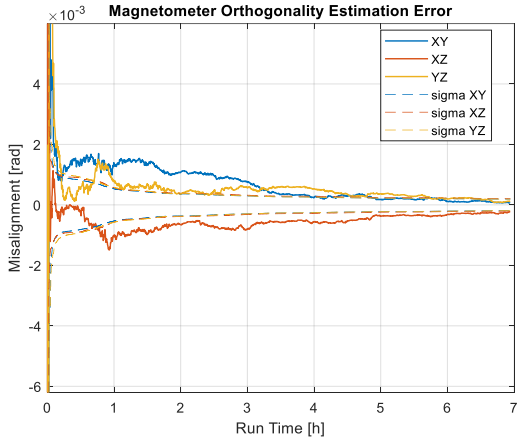

Figure 17 Magnetometer orthogonality estimation error for integrated measurements KF with complex model

Figure 17 shows comparable performance in terms of estimating magnetometer orthogonality errors compared to the regular KF.

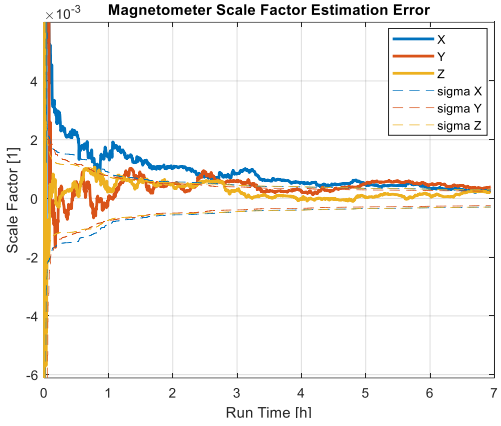

Figure 18 Magnetometer scale factor estimation error for integrated measurements KF with complex model

Figure 18 shows a slight improvement over the regular KF approach in estimating the scale factor error. The residual scale factor is significantly smaller compared to the regular KF.

For the complex model and sensors errors, the speed up of 10s integrated measurements KF was 2.4x. The upper limit without impacting the performance was found to be 20s, which yielded a total speed up of a factor of 2.8x.

5. Conclusion

In this study, a different approach to reducing the computational load of on-board attitude estimation algorithms was proposed. Realistic random sets of sensor data were generated on a LEO trajectory, which were used to demonstrate the estimation performance of the proposed method. Also, method was shown to be lighter overall in a realistic setting.

In conclusion, the integrated measurements approach is a lighter yet as performant replacement to the regular approach.

Further improvements could be obtained combining integrated measurements method with other methods available[13] that are compatible with the problem at hand.

References

1. Pham, M. D., Low, K. S., Goh, S. T., & Chen, S. (2015). Gain-scheduled extended Kalman filter for Nanosatellite Attitude Determination System. *IEEE Transactions on Aerospace and Electronic Systems*, *51*(2), 1017–1028. https://doi.org/10.1109/taes.2014.130204
2. Chia, J. W., Tissera, M. S., Low, K. S., Goh, S. T., & Xing, Y. T. (2016). A low complexity Kalman filter for improving MEMS based gyroscope performance. *2016 IEEE Aerospace Conference*. https://doi.org/10.1109/aero.2016.7500795
3. Guivant José E. (2002). *Efficient simultaneous localization and mapping in large environments* (thesis).
4. Bonato, V., Marques, E., & Constantinides, G. A. (2008). A floating-point extended Kalman filter implementation for Autonomous Mobile Robots. *Journal of Signal Processing Systems*, *56*(1), 41–50. https://doi.org/10.1007/s11265-008-0257-8
5. Savage, P. G. (2007). Chapter 3, 6. In *Strapdown Analytics*., Strapdown Associates.
6. Kalman, R. E. (1960). A new approach to linear filtering and prediction problems. *Journal of Basic Engineering*, *82*(1), 35–45. https://doi.org/10.1115/1.3662552
7. Markley, F. L. (2003). Attitude error representations for Kalman filtering. *Journal of Guidance, Control, and Dynamics*, *26*(2), 311–317. https://doi.org/10.2514/2.5048
8. Titterton, D. H., & Weston, J. L. (2004). In *Strapdown Inertial Navigation Technology* (p. 195). essay, Institution of Electrical Engineers.
9. Steyn, W. H. (2020). Stability, pointing, and orientation. *Handbook of Small Satellites*, 145–187. https://doi.org/10.1007/978-3-030-36308-6_8
10. Ivanov, D., Ovchinnikov, M., Ivlev, N., & Karpenko, S. (2015). Analytical study of microsatellite attitude determination algorithms. *Acta Astronautica*, *116*, 339–348. https://doi.org/10.1016/j.actaastro.2015.07.001
11. Hajiyev, C. (2015). Orbital calibration of microsatellite magnetometers using a linear Kalman filter. *Measurement Techniques*, *58*(9), 1037–1043. https://doi.org/10.1007/s11018-015-0838-4
12. Inamori, T., Sako, N., & Nakasuka, S. (2010). Strategy of magnetometer calibration for nano-satellite missions and in-orbit performance. *AIAA Guidance, Navigation, and Control Conference*. https://doi.org/10.2514/6.2010-7598
13. Raitoharju, M., & Piche, R. (2019). On computational complexity reduction methods for Kalman filter extensions. *IEEE Aerospace and Electronic Systems Magazine*, *34*(10), 2–19. https://doi.org/10.1109/maes.2019.2927898